RADC-TR-78-214
Final Technical Report
October 1978

A COMPARISON OF VARIOUS RESTORATION TECHNIQUES

J. F. Belsher
J. W. Goodman

Stanford University

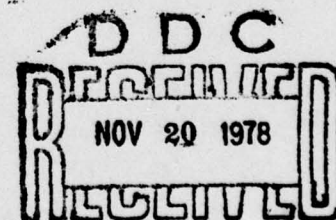Approved for public release; distribution unlimited.

ROME AIR DEVELOPMENT CENTER
Air Force Systems Command
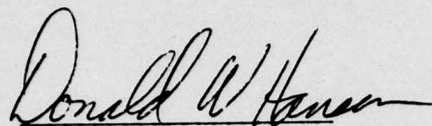Griffiss Air Force Base, New York   13441

78 11 17 082

This report has been reviewed by the RADC Information Office (OI) and is releasable to the National Technical Information Service (NTIS). At NTIS it will be releasable to the general public, including foreign nations.

RADC-TR-78-214 has been reviewed and is approved for publication.

APPROVED:

DONALD W. HANSON
Project Engineer

MISSION
of
Rome Air Development Center

RADC plans and conducts research, exploratory and advanced
development programs in command, control, and communications
(C^3) activities, and in the C^3 areas of information sciences
and intelligence. The principal technical mission areas
are communications, electromagnetic guidance and control,
surveillance of ground and aerospace objects, intelligence
data collection and handling, information system technology,
ionospheric propagation, solid state sciences, microwave
physics and electronic reliability, maintainability and
compatibility.

REPORT DOCUMENTATION PAGE		READ INSTRUCTIONS BEFORE COMPLETING FORM
1. REPORT NUMBER RADC-TR-78-214	2. GOVT ACCESSION NO.	3. RECIPIENT'S CATALOG NUMBER
4. TITLE (and Subtitle) A COMPARISON OF VARIOUS RESTORATION TECHNIQUES.		5. TYPE OF REPORT & PERIOD COVERED Final Technical Report, 1 Oct 77 - 1 Jul 78,
		6. PERFORMING ORG. REPORT NUMBER N/A
7. AUTHOR(s) J. F. Belsher J. W. Goodman		8. CONTRACT OR GRANT NUMBER(s) F30602-75-C-0228, ARPA Order-2646
9. PERFORMING ORGANIZATION NAME AND ADDRESS Stanford University Stanford CA 94305		10. PROGRAM ELEMENT, PROJECT, TASK AREA & WORK UNIT NUMBERS 62301E 26460405
11. CONTROLLING OFFICE NAME AND ADDRESS Defense Advanced Research Projects Agency 1400 Wilson Blvd Arlington VA 22209		12. REPORT DATE October 1978
		13. NUMBER OF PAGES 39
14. MONITORING AGENCY NAME & ADDRESS(if different from Controlling Office) Rome Air Development Center (OCSE) Griffiss AFB NY 13441		15. SECURITY CLASS. (of this report) UNCLASSIFIED
		15a. DECLASSIFICATION/DOWNGRADING SCHEDULE N/A

16. DISTRIBUTION STATEMENT (of this Report)

Approved for public release; distribution unlimited.

17. DISTRIBUTION STATEMENT (of the abstract entered in Block 20, if different from Report)

Same

18. SUPPLEMENTARY NOTES

RADC Project Engineer: Donald W. Hanson (OCSE)

19. KEY WORDS (Continue on reverse side if necessary and identify by block number)

Image Processing
Space-Variant Filtering

20. ABSTRACT (Continue on reverse side if necessary and identify by block number)

This report describes the performance of linear space-variant and invariant filters for several input conditions. The performance of the space-variant filters is shown to be better than the space-invariant filters for many conditions of interest. Spatial variations in both the object being viewed and in the transmission medium are included.

DD FORM 1473
1 JAN 73

332550
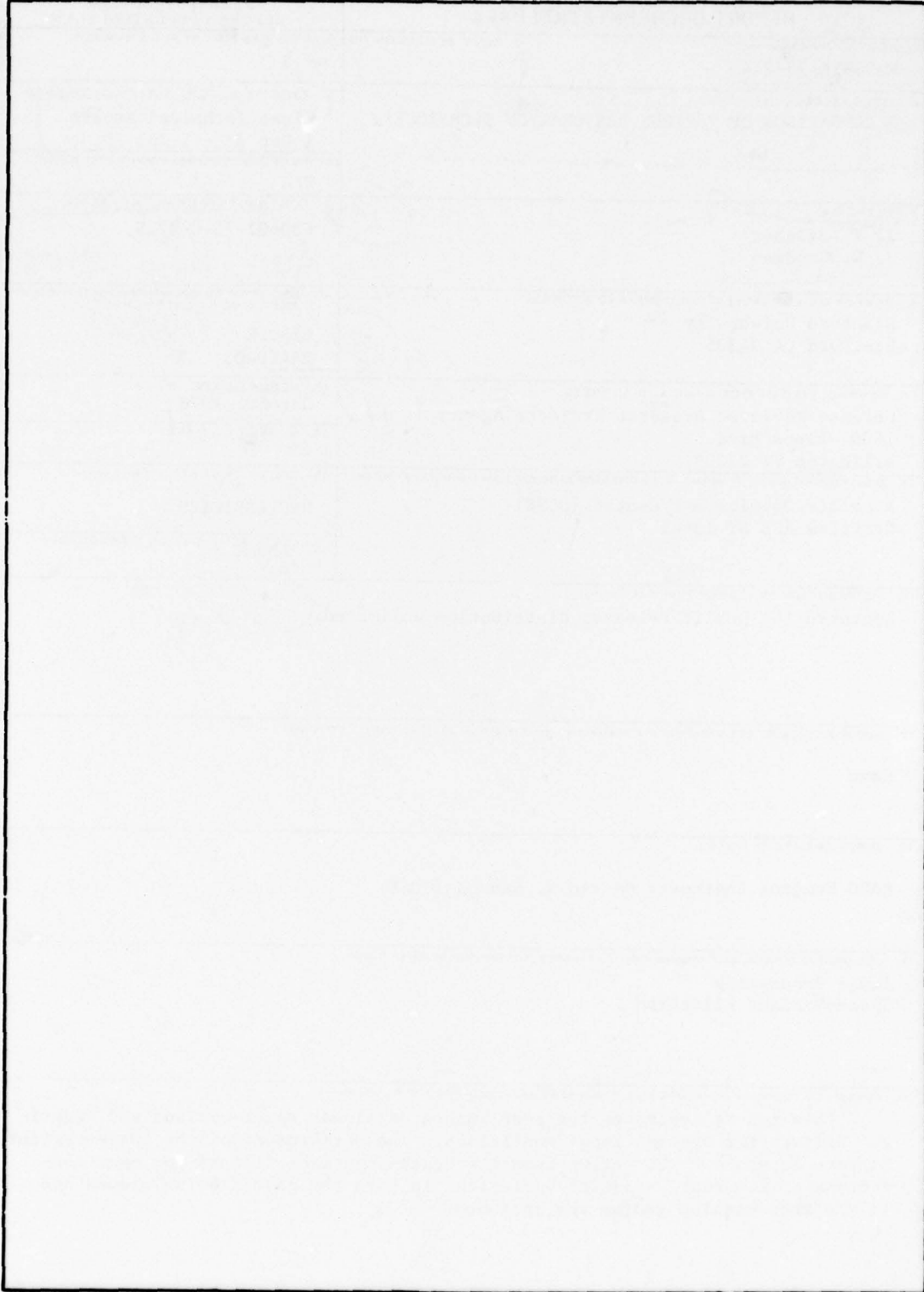
I.   INTRODUCTION

This technical report, which is the last in a series, covers new results in linear restoration of blurred photon-limited images. Our most recent previous technical report [1] is highly recommended as background for this report, and we shall freely call upon results derived there. However, this report does contain a brief review (together with some minor corrections) of the earlier work.

For the purposes of motivation, we should mention at the start why we are interested in space-variant linear restoration of degraded images. Compensated imaging systems correct for atmospheric blur over only a fi-nite field (the so-called "isoplanatic region"). If objects larger than this field are encountered, the blur present in the image will be markedly space-variant. Furthermore, while conventional linear restoration theor-ies assume stationary object statistics, in practice, real ensembles of objects are usually nonstationary in one or more attributes. Both space-variant blurs and nonstationary objects lead to space-variant filtering as a desired approach.

Section II to follow contains the review mentioned above. In Section III, we describe an algorithm for finding a linear restoration filter that maximizes the particular image quality criterion adopted here. Sec-tion IV gives the results of a study of restoring photon-limited images with linear shift-variant restoration filters.

II.   EQUATIONS FOR THE DISCRETE SPACE-VARIANT RESTORATION PROBLEM

As stated above, in this section we give a review of the discrete notation and equations used in our study of space-variant restoration

1

of photon-limited images. During this review, we will show some corrections to the equations given in Section IV of reference 1.

(a) Discrete Notation

The physical process of the formation of an image is modeled by a linear matrix expression. The continuous object radiance distribution is represented by a column vector $\underline{o}$ whose elements are M_o equally spaced samples. The use of lexicographic ordering to represent two-dimensional object and image distributions is discussed in reference 1.

The formation of an image from the object is modeled by the equation

$$\underline{i} = [B] \, \underline{o} \, . \tag{1}$$

Here, the image intensity distribution is represented by the M_i elements of the column vector $\underline{i}$. The blur matrix $[B]$ consists of M_i samples of each of the M_o impulse responses of the imaging-blurring system. In general, the number of samples of the image M_i might not equal the number of samples of the object M_o.

The detected image vector $\underline{d}$ consists of, again in general, M_d elements, each of which represents the photocount from one element of a discrete array of photodetectors. In our work, we have assumed that $M_d = M_i$ and that the nth element d_n of $\underline{d}$ depends directly on only the nth element i_n of $\underline{i}$. In fact, we model the image detection process by assuming that d_n is Poisson distributed with mean rate

$$\lambda_n = \frac{\eta T A}{h \bar{\nu}} \, i_n \, , \tag{2}$$

2

where A is the area of a detector element, and T is the observation interval.

The detected image $\underline{d}$ is restored by linear filtering with the restoration filter $[H]$. This filter will be chosen to make the restored image $\underline{r}$, given by

$$\underline{r} = [H] \, \underline{d} \, , \tag{3}$$

as "close" as possible to an "ideally filtered" object

$$\underline{\tilde{o}} = [\hat{S}] \, \underline{o} \, . \tag{4}$$

Here, $[\hat{S}]$ is an $M_{\tilde{o}} \times M_o$ matrix of samples of the impulse response of an ideal filter. The normalization indicated by $^\wedge$ was defined in reference 1. In general, therefore, the filter $[H]$ is of dimension $M_{\tilde{o}} \times M_d$.

(b) Minimum Mean-Squared-Error Filter

One method of making the restored image $\underline{r}$ "close" to the ideally filtered image $\underline{\tilde{o}}$ is to minimize the mean-squared value of the error column vector $\underline{\epsilon}$ given by

$$\underline{\epsilon} = \underline{\tilde{o}} - \underline{r} = [\hat{S}] \, \underline{o} - [H] \, \underline{d} \, . \tag{5}$$

Thus, we wish to minimize the quantity

$$\mathcal{E} = E\left\{ \underline{\epsilon}^t \underline{\epsilon} \right\} = E\left\{ \mathrm{Tr}(\underline{\epsilon}\,\underline{\epsilon}^t) \right\} \tag{6}$$

where t signifies matrix transpose, E is the statistical expectation operator, and Tr( ) is the matrix trace operation.

Referring to reference 1 for the derivation of the following results, the mean-squared-error, in general, is given by

$$\mathcal{E} = \text{Tr}\left([H]\left(\bar{N}\begin{bmatrix} \ddots & & 0 \\ & [\hat{B}] & \hat{\underline{\hat{o}}} \\ 0 & & \ddots \end{bmatrix} + \bar{N}^2[\hat{B}][\check{\mathcal{R}}_o][\hat{B}]^t\right)[H]^t\right.$$

$$\left. - 2k\bar{N}^2[\hat{S}][\check{\mathcal{R}}_o][\hat{B}]^t[H]^t + k^2\bar{N}^2[\hat{S}][\check{\mathcal{R}}_o][\hat{S}]^t\right). \tag{7}$$

An alternate form of the mean-squared-error actually used in calculations is

$$\mathcal{E} = \text{Tr}\left\{k^2\bar{N}^2[\hat{S}][\check{\mathcal{R}}_o][\hat{S}]^t + \bar{N}\left([H]\left(\begin{bmatrix} \ddots & & 0 \\ & [\hat{B}] & \hat{\underline{\hat{o}}} \\ 0 & & \ddots \end{bmatrix}\right.\right.\right.$$

$$\left.\left.\left. + \bar{N}[\hat{B}][\check{\mathcal{R}}_o][\hat{B}]^t\right) - 2k\bar{N}[\hat{S}][\check{\mathcal{R}}_o][\hat{B}]^t\right)[H]^t\right\}. \tag{8}$$

The appropriate minimum mean-squared-error filter can be found in the literature [2] and is given by

$$[H_{\text{MMSE}}] = k\bar{N}[\hat{S}][\check{\mathcal{R}}_o][\hat{B}]^t\left(\begin{bmatrix} \ddots & & 0 \\ & [\hat{B}] & \hat{\underline{\hat{o}}} \\ 0 & & \ddots \end{bmatrix} + \bar{N}[\hat{B}][\check{\mathcal{R}}_o][\hat{B}]^t\right)^{-1}. \tag{9}$$

This filter will, in general, be space variant and nonsquare, depending on the properties and sizes of $[\hat{S}]$, $[\hat{B}]$, $\hat{\underline{\hat{o}}}$, and $[\check{\mathcal{R}}_o]$.

In order to study the performance of a given restoration filter, some measure of image quality must be defined. We have chosen to define image quality Q by

4

$$Q \triangleq \frac{\delta}{\varepsilon} \tag{10}$$

where ε is the mean-squared-error and δ is the expected signal energy at the output given by

$$\delta \triangleq \bar{N}^2 \mathrm{Tr} \left([H] [\hat{B}] [\check{\mathcal{R}}_o] [\hat{B}]^t [H]^t \right) . \tag{11}$$

Substitution of the minimum mean-squared-error filter $[H_{MMSE}]$ into one of the expressions for mean-squared-error, Eq. (7) or (8), yields the expression for the minimum possible mean-squared-error with linear restoration

$$\varepsilon_{min} = k^2 \bar{N}^2 \, \mathrm{Tr} \left([\hat{S}] [\check{\mathcal{R}}_o] \left([I] - [\hat{B}]^t \left(\begin{bmatrix} & & 0 \\ & [\hat{B}] & \hat{0} \\ 0 & & \end{bmatrix} \right.\right.\right.$$

$$\left.\left.\left. + \bar{N} [\hat{B}] [\check{\mathcal{R}}_o] [\hat{B}]^t \right)^{-1} [\hat{B}] [\check{\mathcal{R}}_o] \right) [\hat{S}]^t \right) . \tag{12}$$

(In reference 1, the corresponding equation, Eq. (36), has a misplaced parenthesis.) In our computations, the alternative form

$$\varepsilon_{min} = k^2 \bar{N}^2 \, \mathrm{Tr} \left([\hat{S}] [\check{\mathcal{R}}_o] [\hat{S}]^t - \frac{1}{k} [H_{MMSE}] [\hat{B}] [\check{\mathcal{R}}_o] [\hat{S}]^t \right) \tag{13}$$

for the minimum mean-squared-error has been used. (The corresponding Eq. (37) in reference 1 has an omission. Note here that the form of Eq. (38) in reference 1 used for comparison to the continuous case is correct only if all matrices in the expression are square, i.e., if $M_o = M_i = M_{\tilde{o}}$. The more generally valid expression, requiring only $M_i = M_{\tilde{o}}$, is

5

$$\mathcal{E}_{min} = k^2 \bar{N}^2 \, \text{Tr} \left([\hat{S}][\check{\mathcal{R}}_o][\hat{S}]^t \left(\begin{bmatrix} & & 0 \\ & [\hat{B}] & \hat{\underline{o}} \\ 0 & & \end{bmatrix} + \bar{N}[\hat{B}][\check{\mathcal{R}}_o][\hat{B}]^t \right)^{-1} \begin{bmatrix} & & 0 \\ & [\hat{B}] & \hat{\underline{o}} \\ 0 & & \end{bmatrix} \right)$$

(14)

which in the square matrix case reduces to Eq. (38), reference 1.)

Thus, we have several forms for the denominator of the expression for Q. For the numerator, we substitute Eq. (9) into Eq. (11), yielding

$$\delta_{MMSE} = k^2 \bar{N}^4 \, \text{Tr} \left([\hat{S}][\check{\mathcal{R}}_o][\hat{B}]^t \left(\begin{bmatrix} & & 0 \\ & [\hat{B}] & \hat{\underline{o}} \\ 0 & & \end{bmatrix} + \bar{N}[\hat{B}][\check{\mathcal{R}}_o][\hat{B}]^t \right)^{-1} \right.$$

$$\left. \cdot \; [\hat{B}][\check{\mathcal{R}}_o][\hat{B}]^t \left(\begin{bmatrix} & & 0 \\ & [\hat{B}] & \hat{\underline{o}} \\ 0 & & \end{bmatrix} + \bar{N}[\hat{B}][\check{\mathcal{R}}_o][\hat{B}]^t \right)^{-1} [\hat{B}][\check{\mathcal{R}}_o][\hat{S}]^t \right).$$

(15)

(In reference 1, Eq. (43) contains an exponent error and Eq. (44) is more correctly written

$$Q_{MMSE} = \frac{\delta_{MMSE}}{\mathcal{E}_{min}} \tag{16}$$

for the minimum mean-squared-error Q.)

As we show in Section III, we can improve on the performance pre-dicted by Eq. (16). Specifically, we can do better than the minimum mean-squared-error filter by using a filter which maximizes the quality factor Q.

III. MAXIMUM IMAGE QUALITY FILTER

Equation (16) is not the maximum obtainable Q using linear restoration techniques. This is true because in minimizing the mean-squared-error we are not necessarily maximizing the ratio of signal to mean-squared error. Thus, we would like to find the filter $[H_{MQ}]$ which maximizes the image quality

$$Q \triangleq \frac{\delta}{\varepsilon} \, . \tag{10}$$

By following a procedure similar to that used for finding the minimum mean-squared-error filter (see Appendix A), two necessary conditions are found for any $[H_{MQ}]$ producing a local maximum in Q:

$$\frac{\bar{N}^2 \, \mathrm{Tr}\left(2\,[H_{MQ}]\,[\hat{B}]\,[\check{\mathcal{R}}_o]\,[\hat{B}]^t\,[G]^t\right)}{\delta} = \frac{\mathrm{Tr}\left(2\,[H_{MQ}]\,[D]\,[G] - 2k\bar{N}^2\,[G]\,[\hat{B}]\,[\check{\mathcal{R}}_o]\,[\hat{S}]^t\right)}{\varepsilon} \tag{17}$$

and

$$-\frac{2\bar{N}Q_{max}\, \mathrm{Tr}\left([G]\left(\begin{bmatrix} & & & 0 \\ & [\hat{B}] \, \hat{\underline{o}} & \\ 0 & & \end{bmatrix} + \frac{Q_{max} - 1}{Q_{max}}\,\bar{N}\,[\hat{B}]\,[\check{\mathcal{R}}_o]\,[\hat{B}]^t\right)[G]^t\right)}{\varepsilon} < 0 \tag{18}$$

for all matrices $[G]$, where in (17) expressions (7) and (11) have been used and

$$[D] = \left(\begin{bmatrix} & & & 0 \\ & [\hat{B}] \, \hat{\underline{o}} & \\ 0 & & \end{bmatrix} + \bar{N}\,[\hat{B}]\,[\check{\mathcal{R}}_o]\,[\hat{B}]^t\right) \, . \tag{19}$$

7

By rearranging terms, we find that condition (17) will be satisfied if and only if

$$[H_{MQ}] = k\bar{N}[\hat{S}][\check{\mathcal{R}}_o][\hat{B}]^t \left(\begin{bmatrix} & & & 0 \\ & [\hat{B}] & \hat{\underline{o}} & \\ 0 & & & \end{bmatrix} + \bar{N}\left(\frac{Q_{max} - 1}{Q_{max}}\right) [\hat{B}][\check{\mathcal{R}}_o][\hat{B}]^t \right)^{-1} \quad (20)$$

and condition (18) if and only if (20) and

$$\begin{bmatrix} & & & 0 \\ & [\hat{B}] & \hat{\underline{o}} & \\ 0 & & & \end{bmatrix} + \frac{Q_{max} - 1}{Q_{max}} \bar{N}[\hat{B}][\check{\mathcal{R}}_o][\hat{B}]^t > [0] \quad (21)$$

are satisfied, where [0] is a matrix of all zero elements. The inequality (21), for our purposes, is simply an added condition which must be satisfied by any Q_{max} satisfying (20). It is no help to us in finding our maximum Q filter. Note that, if the factor $(Q_{max}-1)/Q_{max}$ is regarded as a simple constant, the maximum Q filter differs from the minimum mean-squared-error filter only by this simple internal parameter.

Equation (20) is not a true solution for the elusive maximum Q filter since it is necessary to know a priori the value of Q_{max}, and in our studies we need $[H_{MQ}]$ to find Q_{max}. In a real image restoration system, however, this might not be a problem, as $[H_{MQ}]$ might, for example, be determined experimentally from the minimum mean-squared-error filter by manually adjusting the factor $(Q_{max}-1)/Q_{max}$. It should be mentioned here that, not only is it difficult to find a filter satisfying (20) and (21), but these are only necessary conditions for the maximum Q filter. These conditions guarantee only a local maximum in the Q-[H] space.

8

For the purposes of this study we have developed a procedure for finding the locally maximum Q filter $[H_{MQ}]$. The procedure may be described as solving the following pair of recursive equations:

$$\frac{1}{k\bar{N}} [H_i] = [\hat{S}][\check{\mathcal{R}}_o][\hat{B}]^t \left(\begin{bmatrix} & & 0 \\ & [\hat{B}] & \hat{\underline{0}} \\ 0 & & \end{bmatrix} + \bar{N}\left(\frac{Q_{i-1} - 1}{Q_{i-1}}\right) [\hat{B}][\check{\mathcal{R}}_o][\hat{B}]^t \right)^{-1}$$

(22)

and

$$Q_i = \bar{N}^2 \frac{\text{Tr}\left(\frac{1}{k\bar{N}} [H_i][\hat{B}][\check{\mathcal{R}}_o][\hat{B}]^t \frac{1}{k\bar{N}} [H_i]^t\right)}{\text{Tr}\left([\hat{S}][\check{\mathcal{R}}_o][\hat{S}]^t + \bar{N}\left(\frac{1}{k\bar{N}} [H_i][D] - 2[\hat{S}][\check{\mathcal{R}}_o][\hat{B}]^t\right) \frac{1}{k\bar{N}} [H_i]^t\right)} .$$

(23)

The solution is reached by performing these steps:

(1) Choose an initial value Q_o by some method. (For this Q_o, one might use the value of Q obtained by using the space-variant or space-invariant minimum mean-squared-error filter, or one might try several values for Q_o and choose that value which produces the largest Q_1. Our experience is that, in most cases, a value of Q_o slightly more than unity works well.)

(2) Find $[H_1]$ from Eq. (22).

(3) Use $[H_1]$ to compute Q_1 using Eq. (23).

(4) Repeat steps 2 and 3 always using the latest Q_i for the next cycle.

(5) Stop when the values of Q_i are no longer increasing.

(6) Check to insure a maximum rather than an inflection point by entering Eqs. (22) and (23) with several values of Q_{i-1} on both sides of the final Q_i from step 4.

9

We have found, using this procedure, solutions for the maximum Q
filter much more easily than we had expected when the procedure was first
proposed. Also, although we have no guarantee that we have found the
global maximum in the Q-[H] space, we have tested a wide range of val-
ues of the factor $(Q_o-1)/Q_o$ and have never found a Q higher than that
obtained from the maximum Q procedure.

IV. LINEAR SPACE-VARIANT FILTERING RESULTS

In this section, we present results of computer analysis of restored
image quality possible when using linear space-variant restoration tech-
niques. We have used both minimum-mean-squared-error and maximum-Q-algo-
rithm filters. We begin by describing the notation and some of the object
statistics and blur types used through Section IV.

(a) Computation Parameters

In our computer studies, we have treated several types of nonsta-
tionary objects and space-variant blurs. We usually allow either the
object statistics or the blur impulse response to be position dependent,
but not both at once. Later, we will define the exact forms used for
those statistics and impulse responses. At this point, we shall describe
some general assumptions and define the types of space-invariant blur
and stationary object used throughout.

First, in all cases, we have restricted ourselves to one-dimensional
objects. During the period covered by this contract, the speed and stor-
age capabilities of the computer at our disposal were never sufficiently
large to allow two-dimensional image processing. In fact, in nearly all
of our studies, we restricted the image and object sizes to 35 pixels.

10

In only a few cases did we allow object and image sizes to grow to 49 pixels. In these cases, we were checking for object-dependent changes in image quality due to edge effect errors. As the object size grew, all the Q curves shifted upward slightly but always by nearly the same amount.

As we stated in Section II, the sizes of the object, classical intensity image, detected image, and ideal image, M_o, M_i, M_d, and $M_{\tilde{o}}$, respectively, will, in general, be different. This might be true due to the physical realities of the imaging system or because it might be advantageous to choose them so. If, for instance, the impulse responses of the actual blur and ideal blur are assumed to be spatially limited, the sizes of the vectors and matrices are often chosen to retain all available information without suffering any unneeded storage penalty.

In our studies, we have assumed more "realistic" blurs which are band limited rather than space limited. These must necessarily be artificially truncated at a rather arbitrary point, especially with our rather severe space limitations. We therefore have assumed that all vectors have the same dimension and that all matrices are square, that is, that

$$M_o = M_i = M_d = M_{\tilde{o}} = M \tag{24}$$

where M is the assumed matrix and vector dimension. As stated above, for all cases presented here, M = 35.

Briefly, with respect to notation, if vector $\underline{a}$ has elements a_i, then the index i is assumed to run from 1 to M. If matrix [A] has elements $[A]_{ij}$, then the index i runs along a column and j runs along a row from 1 to M.

11

The ideal blur matrix used in all our calculations is a sinc^2 function sampled at the Nyquist rate. This sinc^2 impulse response corresponds to a diffraction-limited one-dimensional aperture function. Explicitly, the ideal filter matrix elements are

$$[S]_{ij} = \left(\frac{\sin\,(\pi(i - j)/2)}{\pi(i - j)/2} \right)^2 . \tag{25}$$

This equation is more simply written

$$[S]_{ij} = \begin{cases} 1 & i = j \\ 0 & i - j \text{ even and } i \neq j \\ \left(\dfrac{2}{\pi(i - j)} \right)^2 & i - j \text{ odd} \end{cases} \tag{26}$$

In all our calculations, the blur used is a Gaussian blur with a possibly position-dependent width. Explicitly, it is

$$[B]_{ij} = \frac{1}{w\left(j - \left\lceil \frac{M}{2} \right\rceil\right)} \, e^{-\pi \left(\frac{i \,-\, j}{w\left(j - \left\lceil \frac{M}{2} \right\rceil\right)} \right)^2} \tag{27}$$

where $\lceil x \rceil$ means the smallest integer $\geq x$ and $w(x) = W_b$, a constant, whenever a space-invariant blur is specified. The form of $w(x)$ for a space-variant blur will be described later.

In all our work here, for both stationary and nonstationary object ensembles, we assume the covariance matrix is diagonal. That is, we assume the object variation is uncorrelated from point-to-point in the object. For our stationary object ensembles, the autocorrelation matrix is

12

$$[\mathcal{R}_o] = \sigma_o^2 [I] + k^2 \bar{N}^2 \, \hat{1} \, \hat{1}^t \tag{28}$$

where σ_o^2 is the variance of the object, $[I]$ is the identity matrix, and $\underline{1}$ is a vector all of whose elements are unity. We have two degrees of freedom here, the variance and the flux level, and in practice we specify $\bar{N}$ and the object squared-mean to variance ratio Δ at the center, defined by

$$\Delta \triangleq \frac{\bar{o}^{-2}_{\left[\frac{M}{2}\right]}}{[\emptyset_o]_{\left[\frac{M}{2}\right]\left[\frac{M}{2}\right]}} \tag{29}$$

where $\bar{o}_i$ is the ith element of the mean object vector and $[\emptyset_o]$ is the object covariance matrix.

The constant k is defined by

$$k \triangleq \frac{h\bar{\nu}}{b_o \eta TA} \tag{30}$$

where b_o is the net energy transmittance of the imaging process. This constant k has not been specified explicitly in our calculations for two reasons. First, in all our results, we present image quality plotted versus the mean number of photoevents per image rather than versus the total mean object brightness. Thus, we have no need to translate total brightness into total photoevents by using k. Second, we have implicitly assumed that all quantities in Eq. (30) are deterministic and known a priori. Thus, the restoration filter can compensate for the effects of the constant k and effectively remove k from our results.

13

(b) Space-Variant Blur

Here, we show results of restored image quality for situations having stationary object ensembles and space-variant blurs. We use minimum mean-squared-error and maximum Q algorithm restoration filters of both the space-invariant and space-variant types.

The space-variant blur we use is that of Eq. (27) with

$$w(j) = W_c + (W_e - W_c) \frac{\left| j - \left\lceil \frac{M}{2} \right\rceil \right|}{\left\lceil \frac{M}{2} \right\rceil} \tag{31}$$

where W_c and W_e are the widths at the center and edge, respectively. A parabolic width function was also tested, and the results were very similar to those presented here.

Figure 1 shows Q vs $\log_{10} \bar{N}$ for several images restored with minimum mean-squared-error filters. In part (a), the central object mean-to-variance ratio Δ is 1 and, in (b), Δ is 20. In both parts, curves are shown for: (1) a space-invariant blur with $W_b = 8$ and with its corresponding space-invariant restoration filter; (2) a slightly space-variant blur with $W_c = 8$ and $W_e = 10$ with a space-variant restoration filter; and (3) a severely space-variant blur of $W_c = 8$ and $W_e = 16$ also with a space-variant restoration filter. These curves represent the best one can do with linear minimum mean-squared-error restoration applied to these particular blurs. The Q values decrease, progressing from (1) through (3) in each part because, for a given $\bar{N}$, the filter cannot restore an image as well for larger average blurs.
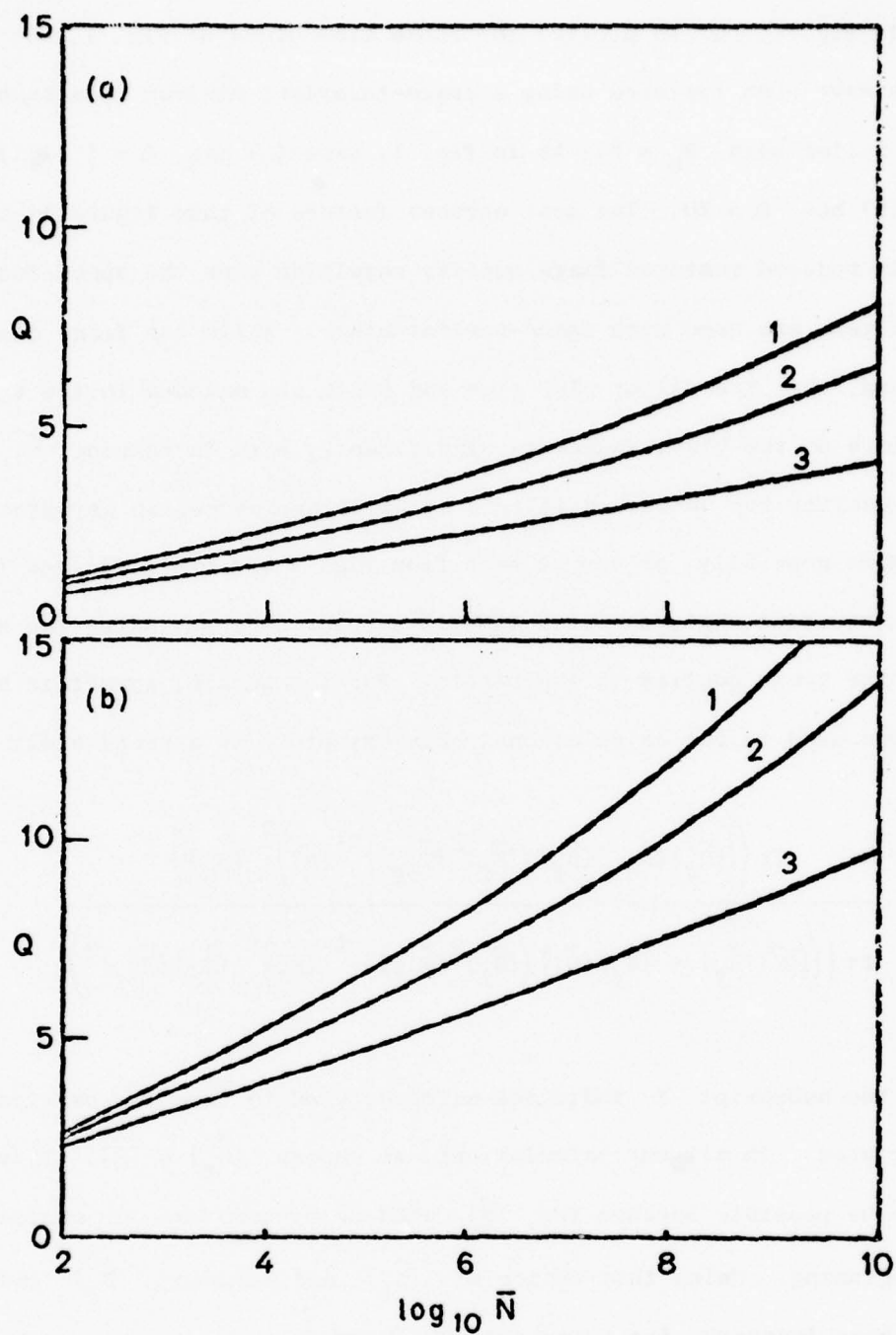
14

Fig. 1. Q vs $\log_{10} \bar{N}$ with minimum mean-squared-error
   filters. Different $\triangle$ values: (a) $\triangle = 1$; (b) $\triangle = 20$.
   Different blurs: (1) space invariant, $W_b = 8$; (2) space
   variant, $W_c = 8$ and $W_e = 10$; (3) space variant,
   $W_c = 8$, $W_e = 16$.

15

In Fig. 2, Q is plotted for those same blurs of Fig. 1, but the images have been restored using a space-invariant minimum mean-squared-error filter with $W_b = 8$. As in Fig. 1, part (a) has $\Delta = 1$ while part (b) has $\Delta = 20$. The most obvious feature of this figure is the greatly reduced restored image quality resulting when the space-invariant filters are used with space-variant blurs. While the image quality obtained, when the filter-blur type and width are matched to the type and width of the blur, increases significantly with increasing $\bar{N}$, the image quality for unmatched filters actually approaches an asymptote.

More generally, as can be seen from Fig. 2 and other figures to follow, we find that, whenever the filter blur does not match the actual blur, the image quality is asymptotic. For the square, symmetric blur matrices used in our calculations, this asymptote is approximately

$$\frac{\text{Tr}\left(\left([\hat{S}_f][\check{\mathcal{R}}_{of}][\hat{B}_f]\left([\hat{B}_f]^2[\check{\mathcal{R}}_{of}]\right)^{-1}[\hat{B}]\right)^2 [\check{\mathcal{R}}_o]\right)}{\text{Tr}\left(\left(\left([\hat{S}][\hat{B}_f] - [\hat{S}_f][\hat{B}]\right)\left([\hat{B}_f]^2[\check{\mathcal{R}}_{of}]\right)^{-1}[\hat{B}]\right)^2 [\check{\mathcal{R}}_o][\check{\mathcal{R}}_{of}]^2\right)}
\tag{32}$$

where the subscript f indicates matrices used to form the particular filter used. In all our calculations, we choose $[\hat{S}_f] = [\hat{S}]$. This will always be possible because the $[\hat{S}]$ used everywhere was our choice in the beginning. Using this choice of $[\hat{S}_f]$ and assuming $[\hat{B}_f]$ and $[\check{\mathcal{R}}_o]$ have inverses, the asymptote (32) becomes

$$\frac{\text{Tr}\left(\left([\hat{S}][\hat{B}_f]^{-1}[\hat{B}]\right)^2 [\check{\mathcal{R}}_o]\right)}{\text{Tr}\left(\left([\hat{S}]\left([\hat{B}_f] - [\hat{B}]\right)[\hat{B}_f]^{-2}[\hat{B}]\right)^2 [\check{\mathcal{R}}_o]\right)} \, .
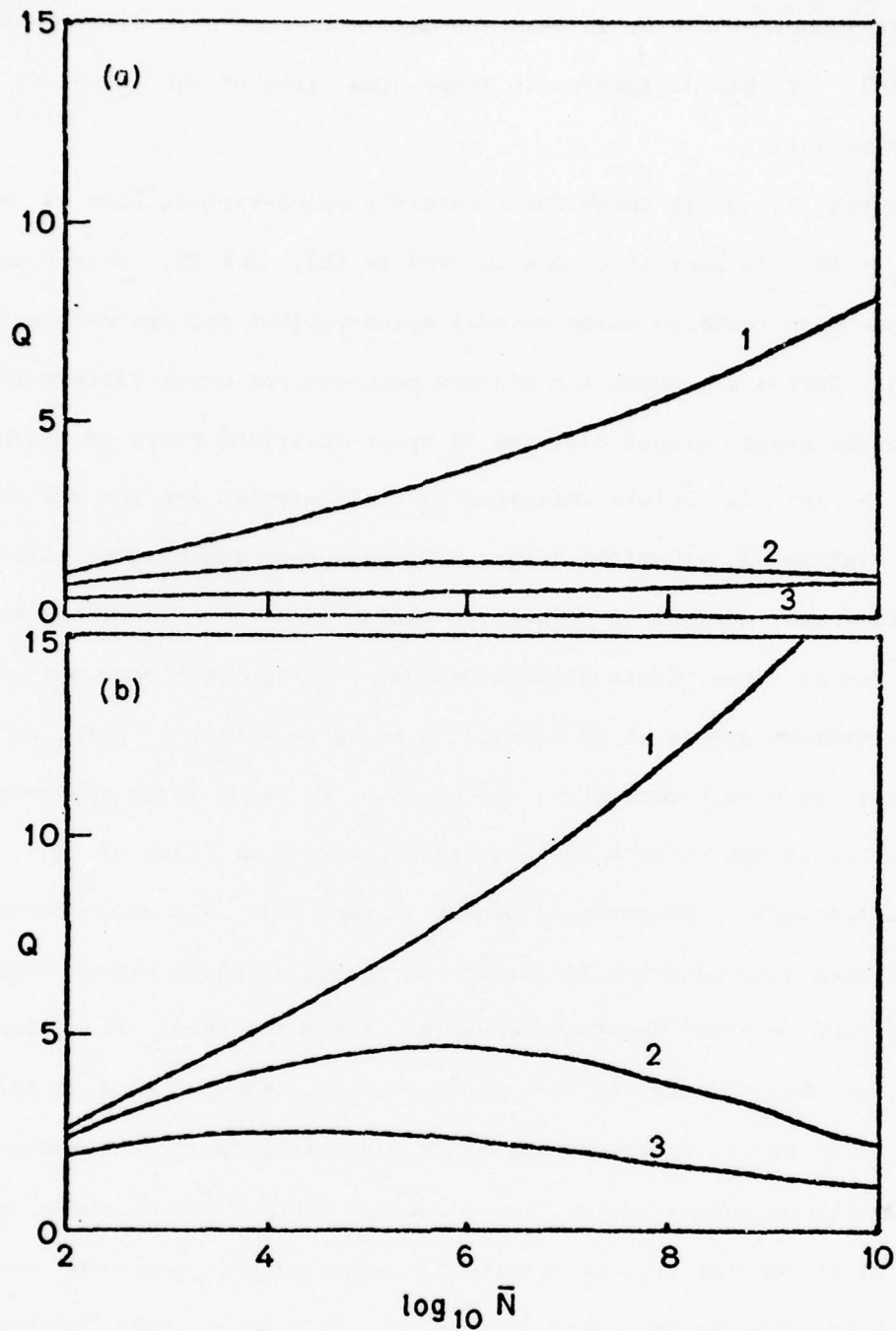\tag{33}$$

16

Fig. 2. Q for restoration with a space-invariant minimum mean-squared-error filter. Two Δ values: (a) $\Delta = 1$; (b) $\Delta = 20$. Different blurs: (1) space invariant, $W_b = 8$; (2) space variant, $W_c = 8$ and $W_e = 10$; (3) space variant, $W_c = 8$, $W_e = 16$.

17

The most important factor in this expression is the "blur difference" $[\hat{B}_f] - [\hat{B}]$. If this difference is large, the value of the asymptote approaches unity.

In Fig. 3, Q is shown for a severely space-variant blur of $W_c = 8$ and $W_e = 16$. In part (a), $\Delta = 1$, and in (b), $\Delta = 20$. This blurred image has been restored using several space-variant and space-invariant filters. Curves are shown for minimum mean-squared-error filters matched both to the space-variant blur and to space-invariant blurs of widths $W_b = 4$, 8, and 12. Points indicated by small circles are for restoration with a maximum Q algorithm filter. Crosses show restoration with a space-invariant maximum Q algorithm filter with $W_b = 8$. There are only a few of these points plotted because the algorithm does not guarantee a maximum unless it is allowed to be space variant. Here, as in most cases we have encountered, the maximum Q value falls approximately one unit above the minimum mean-squared-error filter value of Q.

An interesting phenomenon appears in part (a). The space-invariant minimum mean-squared-error filter has performed slightly better than the space-variant minimum mean-squared-error filter for small $\bar{N}$. Later, in Fig. 5, we shall present an even more pronounced example of this phenomenon. It is not as disconcerting as it might seem to see the space-invariant filter perform better than the space-variant filter since, as we mentioned in Section III, minimizing the mean-squared-error does not necessarily maximize the image quality Q. In a sense, this "better performance" of the space-invariant filter is just an accident. By chance, the mismatched blur has introduced an approximation to the factor $(Q-1)/Q$ of the maximum-Q-algorithm filter. This mismatch could just as well have decreased the effectiveness of the filter.

18
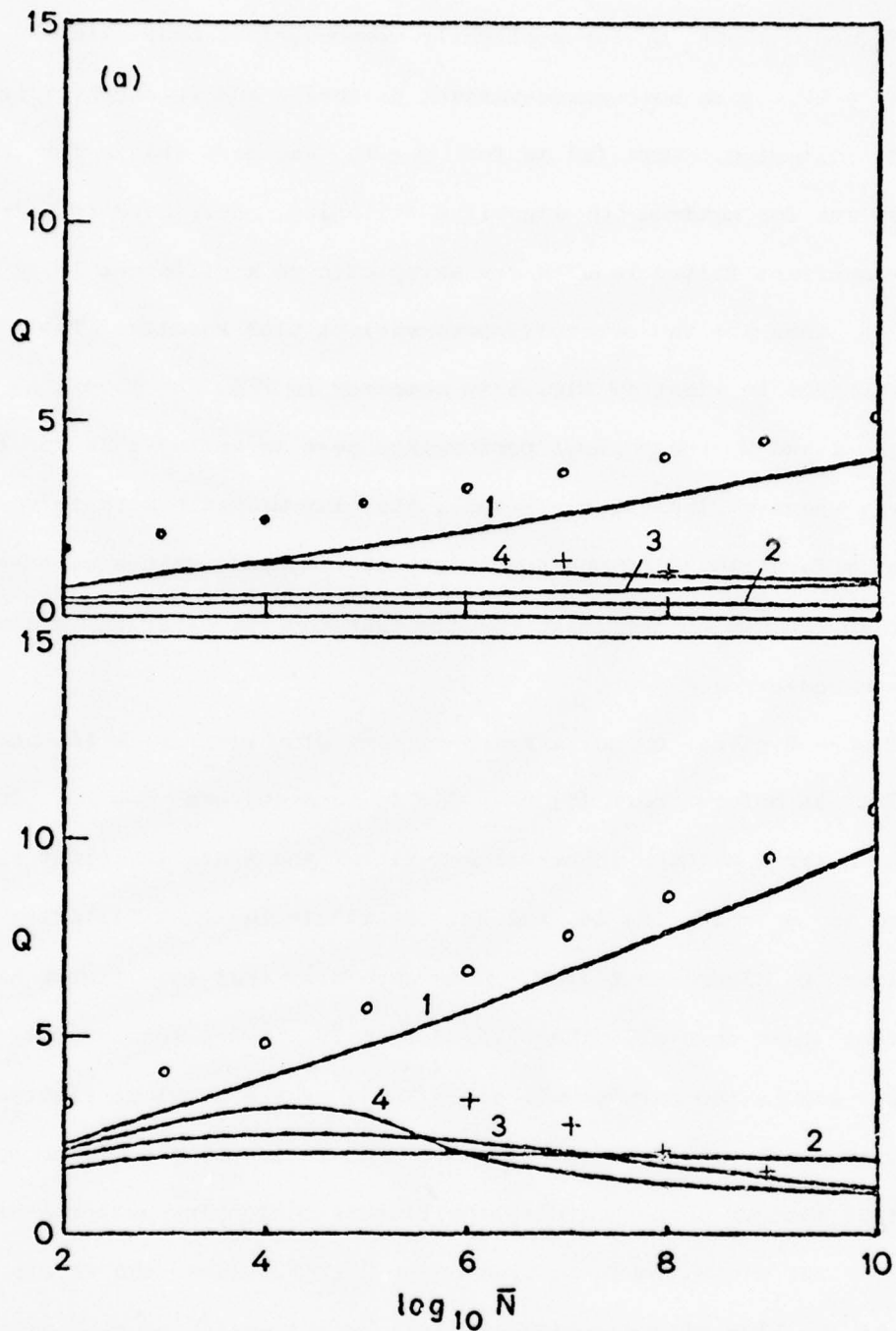
Fig. 3. Q for space-variant, $W_c = 8$ and $W_e = 16$, blur. Two Δ values: (a) $\Delta = 1$; (b) $\Delta = 20$. Several minimum mean-squared-error filters: (1) space variant, $W_c = 8$ and $W_e = 16$; (2) space invariant, $W_b = 4$; (3) space invariant, $W_b = 8$; (4) space invariant, $W_b = 12$. Two maximum-Q-algorithm filters: (○) space variant, $W_c = 8$, $W_e = 16$; (+) space invariant, $W_b = 8$.

19

Figure 4 shows Q for a slightly space-variant blur with $W_c = 8$ and $W_e = 10$, with both space-variant filtering and space-invariant $W_b = 8$ filtering. Part (a) is for $\Delta = 1$, and part (b) is for $\Delta = 20$. Circles are for maximum Q algorithm filtering. Note here that the space-invariant filter results are asymptotic to a different level for large $\bar{N}$ than are the severely space-variant blur results. Two other features come to light if Fig. 4 is compared to Fig. 3. First, as seen in Figs. 1 and 2, the general performance here is better than for the severely space-variant blur. Second, the blur mismatch here is not sufficiently large to allow the space-invariant minimum mean-squared-error filter to produce better image quality than the space-variant minimum mean-squared-error filter.

Figure 5 gives Q for a space-variant blur with $W_c = 16$ and $W_e = 32$. As before, part (a) has $\Delta = 1$, and (b) has $\Delta = 20$. Curves are shown for a matched space-variant filter and space-invariant filters matched to $W_b = 12, 16, 24,$ and 32. Small circles show filtering with a maximum Q algorithm filter. Note carefully that this figure has a different scale than all others in Section IV. Here, the severity of the blur lowers the curves well below those of the previous figures. As mentioned above, in Fig. 5(a) we have a dramatic example of the space-invariant minimum mean-squared-error filters performing better than the space-variant minimum mean-squared-error filter. Here, the severe mismatch of the blur allows good accidental approximation of the maximum Q filter over a range of $\bar{N}$. In addition, the mismatch is enough to force the space-invariant filters' performances to the large $\bar{N}$ asymptote's minimum value of unity.
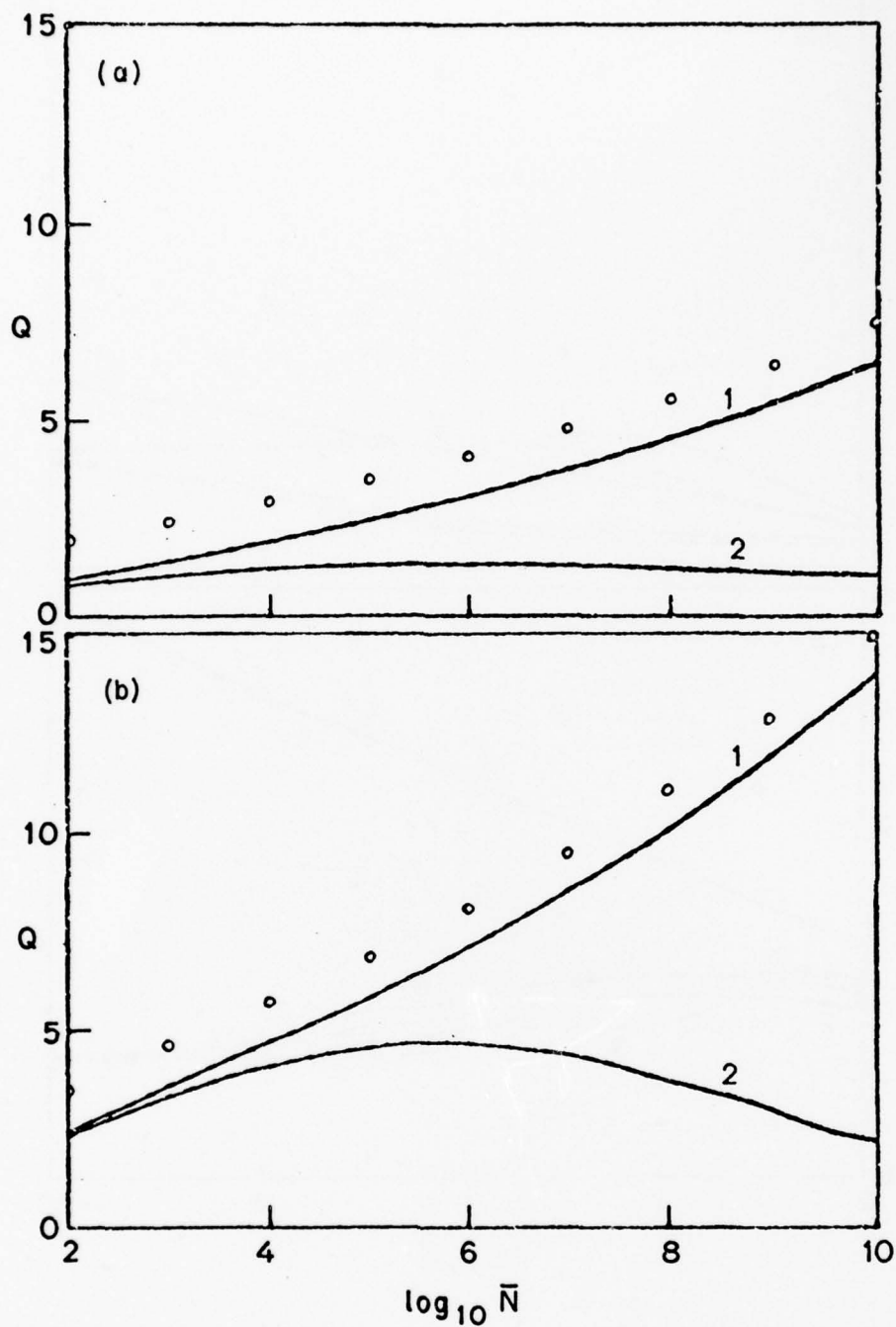
Fig. 4. Q for space-variant, $W_c = 8$ and $W_e = 10$, blur. Two Δ values: (a) $\Delta = 1$; (b) $\Delta = 20$. Several minimum mean-squared-error filters: (1) space variant, $W_c = 8$ and $W_e = 10$; (2) space invariant, $W_b = 8$. Also, (○) maximum Q filter.
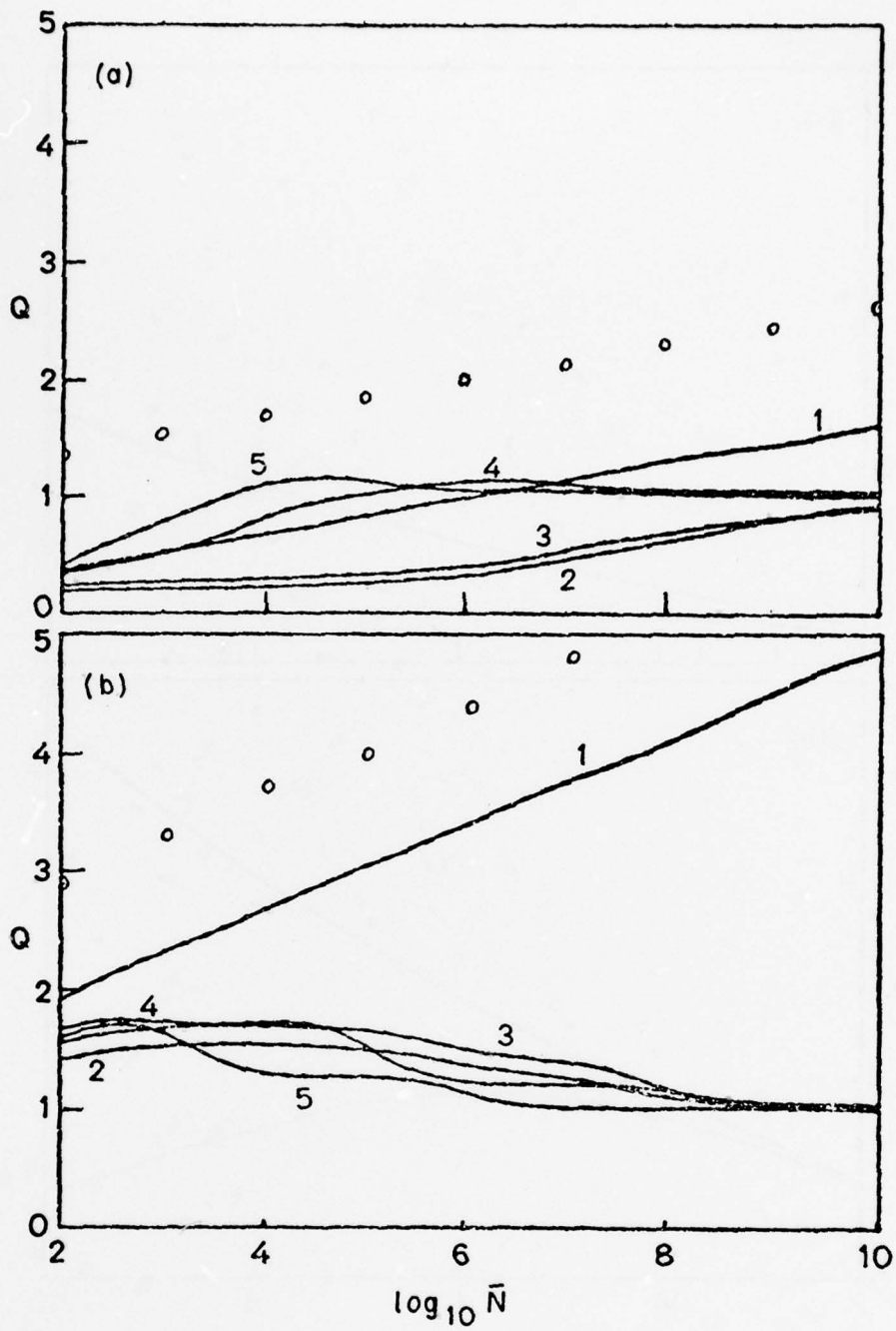
21

Fig. 5. Q for space-variant, $W_c = 16$ and $W_e = 32$, blur. Two Δ values: (a) $\Delta = 1$; (b) $\Delta = 20$. Several minimum mean-squared-error filters: (1) space variant, $W_c = 16$ and $W_e = 32$; (2) space invariant, $W_b = 12$; (3) space invariant, $W_b = 16$; (4) space invariant, $W_b = 24$; (5) space invariant, $W_b = 32$. (○) Maximum Q filtering.

22

(c) <u>Nonstationary Object</u>

Here, we give resulting image quality when nonstationary object en-
sembles are blurred with a space-invariant blur. We study the full range
of minimum mean-squared-error and maximum Q algorithm filters, both
space-variant and space-invariant cases.

We consider two different contributions to the nonstationary sta-
tistics of the object ensemble: the mean and the covariance. We allow
both of these to be position dependent, individually and together. When
we indicate nonstationary mean, we are using $\bar{o}$ of the form

$$\bar{o}_i = \Lambda\left(\frac{i - \left\lceil\frac{M}{2}\right\rceil}{W_o/2}\right) \tag{34}$$

where W_o is an object width parameter and

$$\Lambda(x) = \begin{cases} 1 - |x| & \text{for} \quad |x| \leq 1 \\ 0 & \text{for} \quad |x| > 1 \end{cases}. \tag{35}$$

For those cases where we use a nonstationary covariance, the form is

$$[\emptyset]_{ij} = \begin{cases} 0 & \text{for} \quad i \neq j \\ \Lambda^2\left(\dfrac{i - \left\lceil\frac{M}{2}\right\rceil}{W_o/2}\right) & \text{for} \quad i = j \end{cases} \tag{36}$$

In all of Section IV(c), the blur is space invariant with $W_b = 8$.

Figure 6 shows Q for three different nonstationary object ensem-
bles with $\Delta = 1$. The upper three curves are restored using the appro-
priate space-variant minimum mean-squared-error filters. The lower three

23
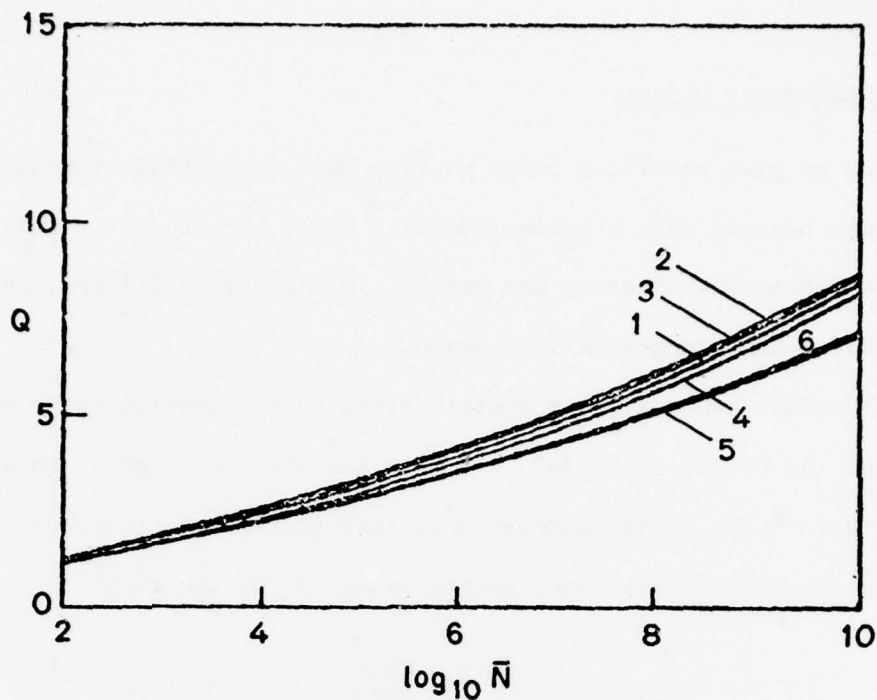
Fig. 6. Q vs $\log_{10} \bar{N}$ for different nonstationary object statistics: (1) & (4) nonstationary mean; (2) & (5) nonstationary covariance; (3) & (6) nonstationary mean and covariance. Different filters used are: (1), (2), & (3) space-variant minimum mean-squared error filters; (4), (5), & (6) space-invariant minimum mean-squared-error filters.
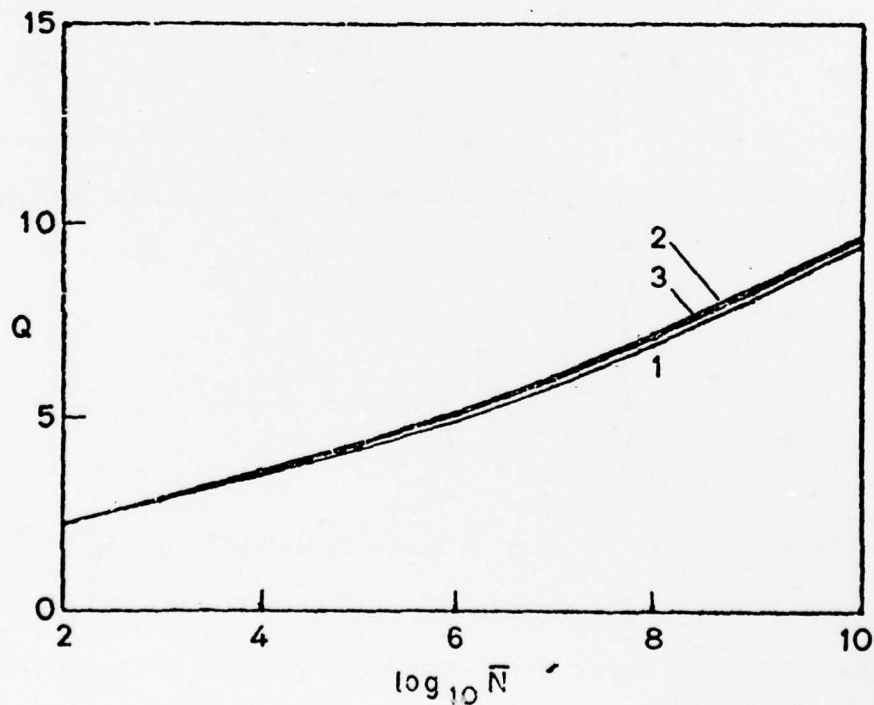

Fig. 7. Q for different nonstationary object statistics: (1) nonstationary mean; (2) nonstationary covariance; (3) nonstationary mean and covariance.

24

curves correspond to restorations obtained using space-invariant minimum mean-squared-error filters. The three curves in each group include an object ensemble with: (1) only the mean nonstationary, (2) with only the variance nonstationary, and (3) with both the mean and variance non-stationary. As can be seen, there is little difference for the three types of nonstationarity. The most pronounced feature of the curves here is the gap between the group of three space-invariant filter curves. The nonstationary mean curve is almost as high as the space-variant filter curves. The two curves showing space-invariant filters used with nonstationary object variances show definitely lower performance.

Figure 7 has curves plotted for the maximum Q filter restoring the three types of nonstationarity listed for Fig. 6. Here, there is even less difference between the performances under different object statistics. The maximum Q algorithm seems to compensate optimally for each of the different object ensembles. Again, the maximum value of Q is approximately one unit higher than the minimum mean-squared-error value.

In Fig. 8, Q is plotted for the mean-only nonstationarity. Part (a) has $\Delta = 1$, and (b) has $\Delta = 20$. The blurred images in each part have been restored using the maximum Q filter and the space-variant and space-invariant minimum mean-squared-error filters. It can be seen from this figure that there is very little difference in performance between the space-variant and space-invariant minimum mean-squared-error filters. This difference does not depend significantly on the value of the object center mean-to-variance ratio Δ, whereas, in earlier figures of space-variant blurs, the loss in performance suffered, when using the space-invariant filter, depended strongly on the value of Δ. As before,
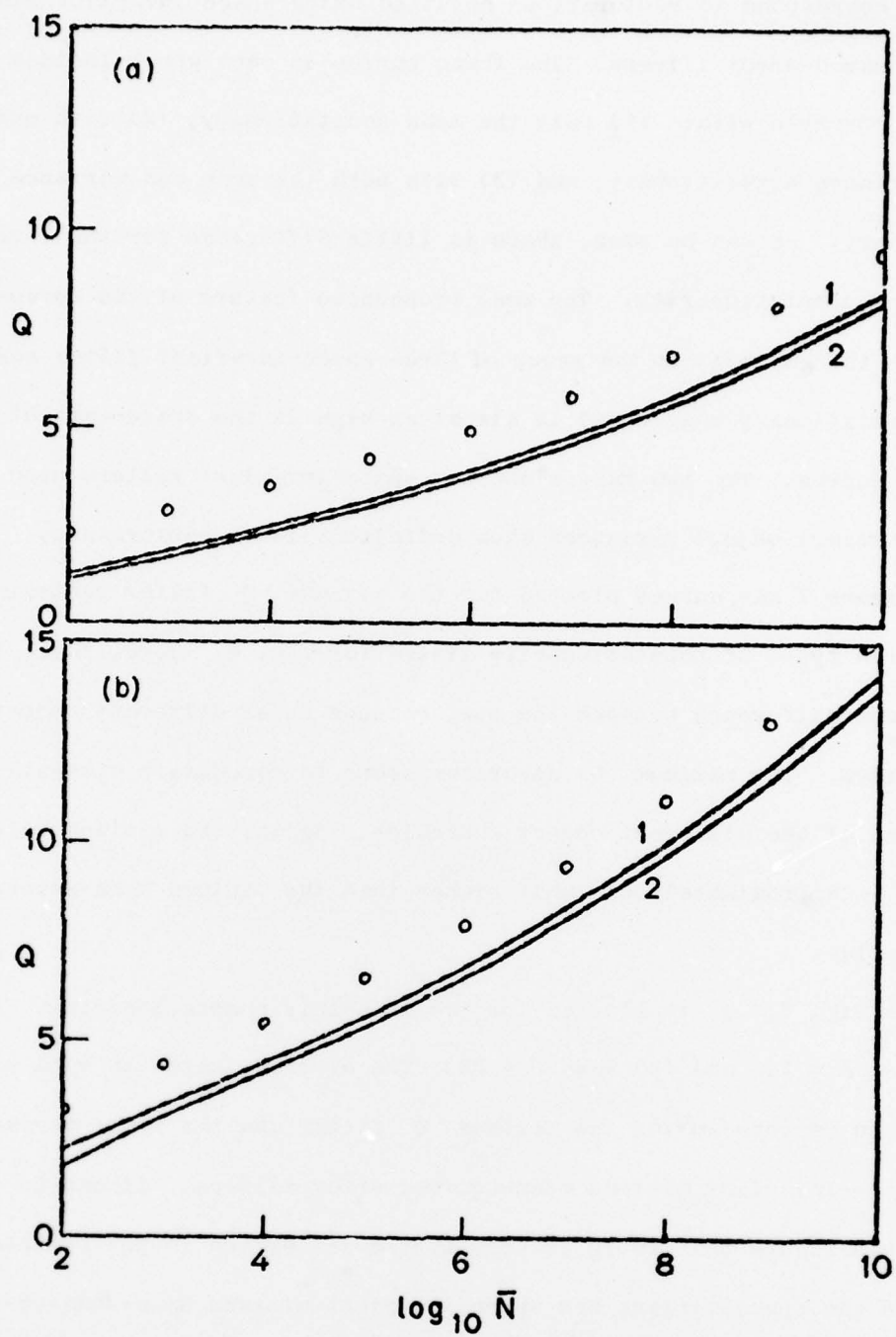
25

Fig. 8. Q for nonstationary object mean. Two Δ values: (a) $\Delta = 1$; (b) $\Delta = 20$. Filters used: (1) minimum mean-squared-error space variant; (2) minimum mean-squared-error space invariant; (○) maximum Q filter.

26

the maximum value of Q is relatively easy to compute and parallels the minimum mean-squared-error Q. Something not seen in this figure is the extreme difficulty in computing a space-invariant maximum-Q-algorithm filter when the variance is stationary.

Figure 9 shows Q plotted for images restored with four filters. These are the space-variant and space-invariant minimum mean-squared-error filters, the maximum Q filter, and the filter derived using the maximum Q algorithm with a space-invariant filter. Part (a) has variance-only nonstationary and part (b) has mean and variance nonstationary. Note here that the crosses, which are the results of space-invariant filtering, show quality comparable to the two space-variant filters. This indicates a computationally workable method of doing useful filtering on nonstationary blurred image ensembles. Here, the maximum Q filter and space-invariant maximum-Q-algorithm filter are both easy to calculate and both parallel their respective minimum mean-squared-error filters in performance.

A further look at Fig. 9 reveals two related points. First, as might be expected, the addition of the nonstationary mean condition of Fig. 8 to the nonstationary variance of Fig. 9(a) leads to a drop in both the maximum Q and the minimum mean-squared-error Q. The levels of Q for the space-invariant maximum-Q-algorithm filter and the minimum mean-squared-error filter are increased by allowing the mean to become nonstationary. This is probably due to "cancelling" errors, another accidental improvement.
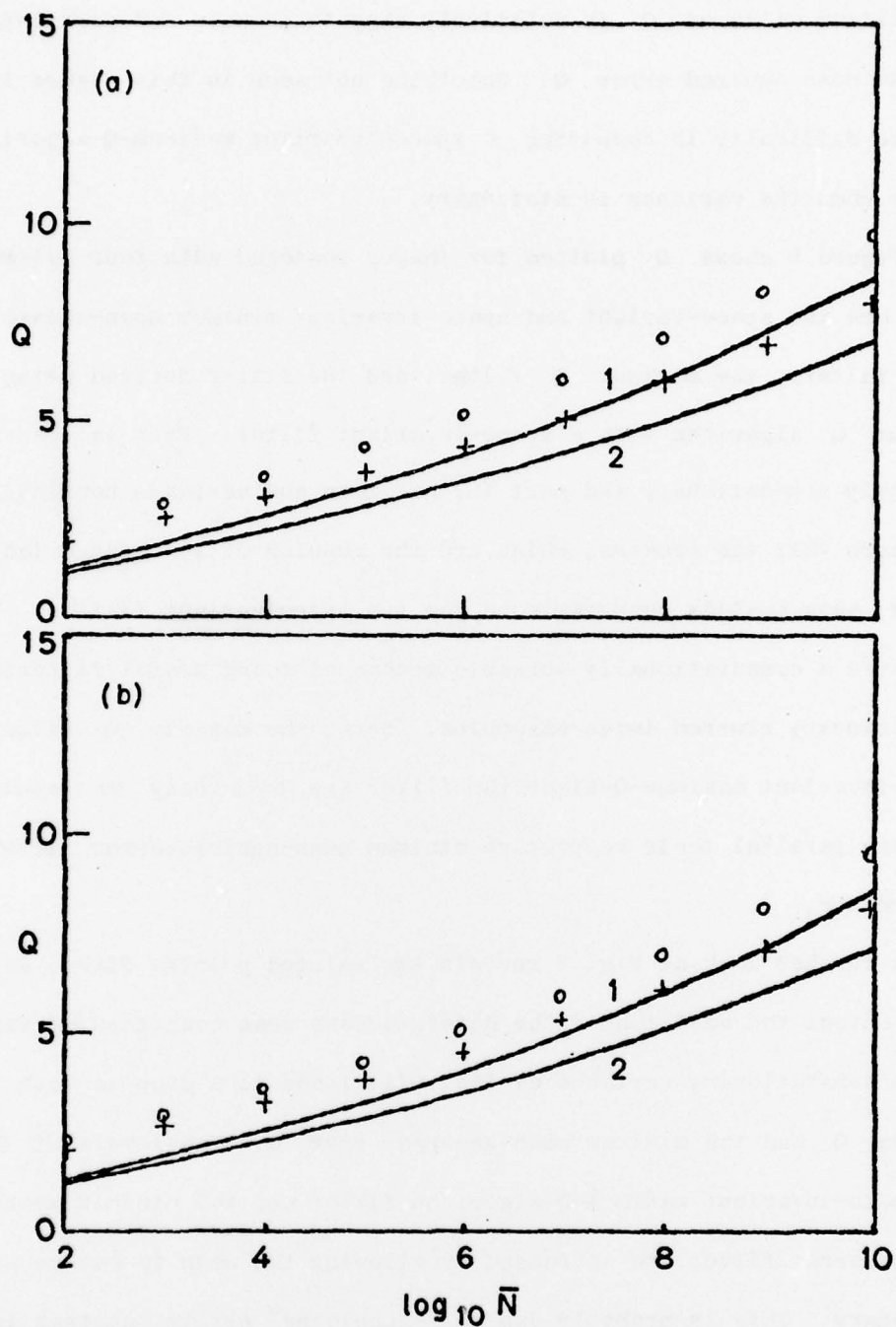
27

Fig. 9. Q for two object statistics: (a) nonstationary covariance; (b) nonstationary mean and covariance. Different filters used: (1) minimum mean-squared-error space variant; (2) minimum mean-squared-error space invariant; (○) maximum Q; (+) maximum-Q-algorithm space invariant.

28

(d) Filter Error Analysis

Often, comments are made to the effect that there are many theoretically good ways to restore degraded images, but they often do not work well due to one's inability to estimate the object statistics and blur impulse responses accurately. We have therefore done the following short study concerning the performance of our filters when they are derived from incorrect statistical or blur response assumptions.

The curves of Fig. 10 show Q for a space-variant blur with $W_c = 8$ and $W_e = 16$. The object ensemble is stationary. Part (a) shows the performance of a space-variant minimum mean-squared-error filter, and part (b) is that for a maximum Q algorithm filter. The three curves in each part include restoration with a properly constructed filter and two restorations with filters constructed with $\pm 10\%$ errors in both W_c and W_e.

In Figs. 11 and 12, a space-invariant blur, $W_b = 8$, is used with an object nonstationary in both mean and variance. In both figures, the filters used are, as in Fig. 10, one accurate filter and one filter with approximately 10% errors in some parameter. In Fig. 11, the error filters have a $\pm 9\%$ error in the object width W_o. In Fig. 12, there is a $\pm 10\%$ error in the blur width W_b.

As can be seen from these figures, an approximately 10% error in the estimated object statistics produces only a few percent reduction in image quality, whereas roughly the same error in estimated blur produces, at least for large $\bar{N}$, a dramatic loss of quality. The basic reason for this dramatic difference is as follows. An error in object statistics affects only the point where the "cutoff" of the Wiener filter occurs.
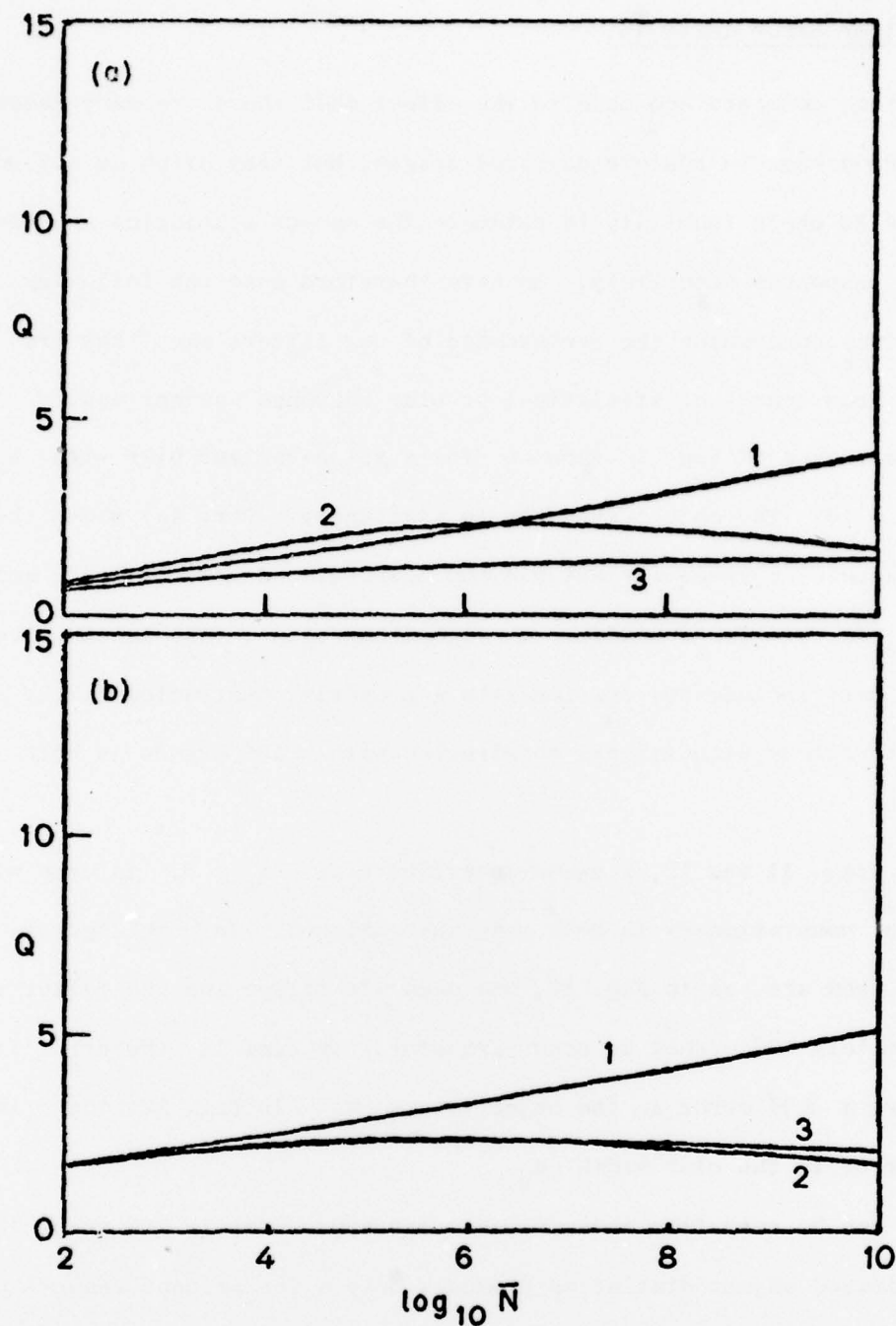
29

Fig. 10. Q for stationary object and space-variant blur, $W_c = 8$ and $W_e = 16$, for mismatched restoration filter. Part (a) minimum mean-squared-error space-variant filter, and part (b) maximum Q filter. In both parts, filter parameters are: (1) $W_c = 8$ and $W_e = 16$; (2) $W_c = 8.8$ and $W_e = 17.6$; (3) $W_c = 7.2$ and $W_e = 14.4$.
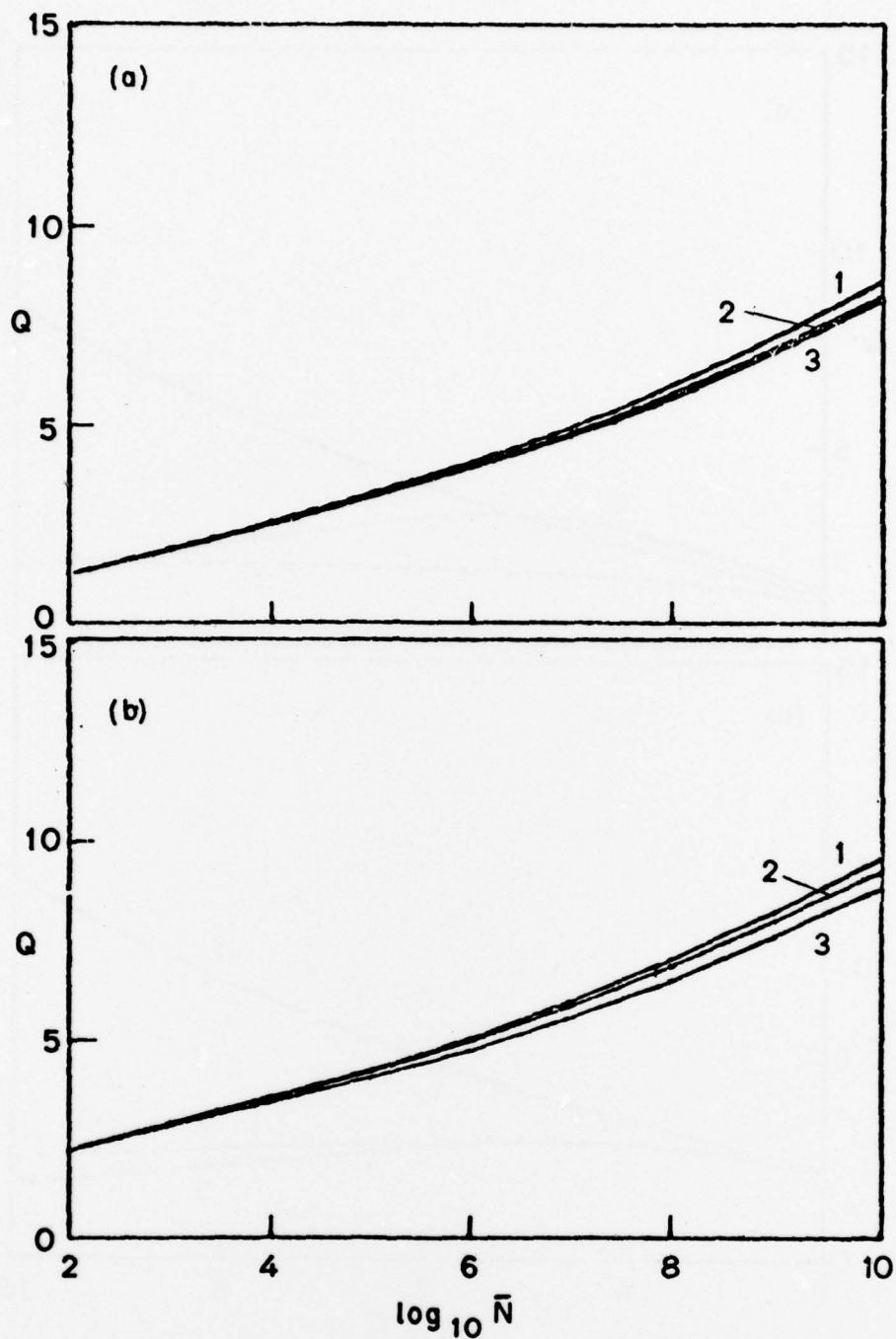
30

Fig. 11. Q for space-invariant $W_b = 8$ blur and nonstationary object mean and covariance, $W_o = 34$, for filter mismatched in object width. Part (a) space-variant minimum mean-squared-error filter, and part (b) maximum Q filter. In both parts, filter parameters are: (1) $W_o = 34$; (2) $W_o = 37.5$; (3) $W_o = 30.5$.
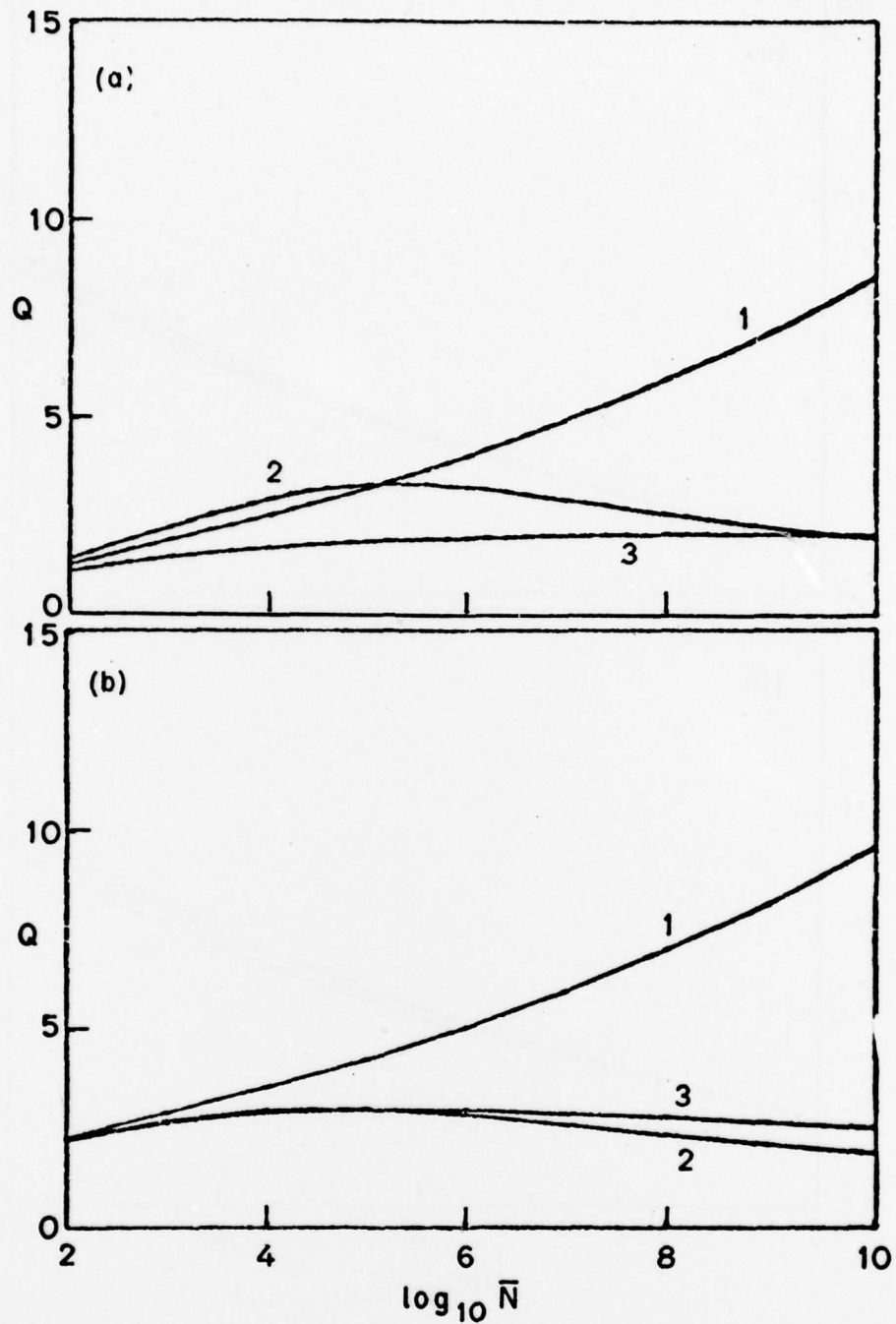
31

Fig. 12. Q for space-variant $W_b = 8$ blur and nonstationary mean and covariance, $W_o = 34$, for filter mismatched in blur width. In part (a) minimum mean-squared-error space-variant filters and part (b) maximum Q filters. In both parts: (1) $W_b = 8$; (2) $W_b = 8.8$; (3) $W_b = 7.2$.

32

This effect should be most pronounced for small $\bar{N}$ where the signal-to-noise ratio is small. The only error this produces is either a loss of signal or increase in noise for those spatial frequencies near the cut-off.

An error in estimating the blur, on the other hand, means that, when $\bar{N}$ becomes large and the Wiener filter approaches an inverse filter, one is only removing a part of the existing blur, or possibly adding additional bur. This effect will be known to anyone familiar with inverse filtering techniques.

This result is somewhat encouraging, however, since, in the atmospheric and compensated imaging systems of interest here, the amount of blur present can be measured with reasonable accuracy while the object statistics are relatively unknown a priori.

APPENDIX A

In this appendix, we derive a set of conditions which a linear filter must satisfy to insure at least a locally maximum value of image quality Q. We begin with the definition of Q in the discrete formulation

$$Q \triangleq \frac{\delta}{\mathfrak{S}} \tag{A.1}$$

where

$$\delta \triangleq \bar{N}^2 \, \text{Tr} \left([H][\hat{B}][\check{\mathcal{R}}_o][\hat{B}]^t [H]^t \right) . \tag{A.2}$$

and

$$\mathfrak{S} = \text{Tr} \left([H] \left(\bar{N} \begin{bmatrix} & & 0 \\ & [\hat{B}] \, \hat{\underline{o}} & \\ 0 & & \end{bmatrix} + \bar{N}^2 [\hat{B}][\check{\mathcal{R}}_o][\hat{B}]^t \right) [H]^t \right.$$
$$\left. - 2k\bar{N}^2 [\hat{S}][\check{\mathcal{R}}_o][\hat{B}]^t [H]^t + k^2\bar{N}^2 [\hat{S}][\check{\mathcal{R}}_o][\hat{S}]^t \right) . \tag{A.3}$$

The procedure we shall follow here is to assume a form for an arbitrary filter [H] which includes a scalar parameter t. We then find the first and second partial derivatives of Q with respect to t and ɔose appropriate conditions on these to guarantee a local maximum in Q. In order to simplify the maximization procedure, the quantity log Q will be maximized instead of Q itself. This is permissible for $Q \neq 0$ since the logarithm is a monotonically increasing function.

If $[H_{MQ}]$ is the restoration filter which produces a maximum image quality Q_{max}, then any arbitrary filter [H] may be written

34

$$[H] = [H_{MQ}] + t[G] \qquad\qquad (A.4)$$

where t is a scalar and $[G]$ is some matrix. A necessary condition for an extremum or point-of-inflection in Q is

$$\left. \frac{\partial \log Q}{\partial t} \right|_{t=0} = 0 \qquad \forall [G] \qquad\qquad (A.5)$$

where $\forall$ means "for all," and a necessary condition for a maximum is

$$\left. \frac{\partial^2 \log Q}{\partial t^2} \right|_{t=0} < 0 \qquad \forall [G] \; . \qquad\qquad (A.6)$$

Beginning with condition (A.5), it is first useful to note that

$$\log Q = \log \delta - \log \mathcal{E} \; . \qquad\qquad (A.7)$$

Substituting (A.4) into (A.3) and (A.2), and taking the derivative of the logarithms gives

$$\frac{\partial \log Q(t)}{\partial t} = \frac{2\bar{N}^2 \, \text{Tr}\left([H_{MQ}][\hat{B}][\check{\mathcal{R}}_o][\hat{B}]^t[G]^t + t[G][\hat{B}][\check{\mathcal{R}}_o][\hat{B}]^t[G]^t\right)}{\delta(t)}$$

$$- \frac{2\text{Tr}\left([H_{MQ}][D][G]^t + t[G][D][G]^t - k\bar{N}^2[G][\hat{B}][\check{\mathcal{R}}_o][\hat{S}]^t\right)}{\mathcal{E}(t)}$$

$$\qquad\qquad (A.8)$$

where $Q(\cdot)$, $\delta(\cdot)$, and $\mathcal{E}(\cdot)$ indicate the values of Q, δ, and $\mathcal{E}$, respectively, with $t = \cdot$. Letting t approach zero gives

35

$$\frac{\partial \log Q(t)}{\partial t}\bigg|_{t=0} = \frac{2\bar{N}^2 \, \text{Tr}\left([H_{MQ}][\hat{B}][\check{\mathcal{R}}_o][\hat{B}]^t [G]^t\right)}{\delta(t=0)}$$

$$- \frac{2\text{Tr}\left([H_{MQ}][D][G] - k\bar{N}^2[G][\hat{B}][\check{\mathcal{R}}_o][\hat{S}]^t\right)}{\delta(t=0)} = 0 \qquad \forall [G]$$

(A.9)

This resulting condition (A.9) will be satisfied if

$$[H_{MQ}]\left(\begin{bmatrix} & & 0 \\ & [\hat{B}] \hat{\underset{\sim}{0}} & \\ 0 & & \end{bmatrix} + \bar{N}\left(\frac{Q_{max}-1}{Q_{max}}\right)[\hat{B}][\check{\mathcal{R}}_o][\hat{B}]^t\right) - k\bar{N}[\hat{S}][\check{\mathcal{R}}_o][\hat{B}]^t = [0]$$

(A.10)

where [0] is a matrix with all zero elements and again

$$Q_{max} = Q(0) = \frac{\delta(0)}{\delta(0)} .$$

(A.11)

This analysis leads to the following expression for the maximum Q filter:

$$[H_{MQ}] = k\bar{N}[\hat{S}][\check{\mathcal{R}}_o][\hat{B}]^t\left(\begin{bmatrix} & & 0 \\ & [\hat{B}] \hat{\underset{\sim}{0}} & \\ 0 & & \end{bmatrix} + \bar{N}\left(\frac{Q_{max}-1}{Q_{max}}\right)[\hat{B}][\check{\mathcal{R}}_o][\hat{B}]^t\right)^{-1}$$

(A.12)

Here, it must be remembered that Q_{max} in most cases is not known without first knowing $[H_{MQ}]$. This filter is sure to produce a local extremum or point of inflection in Q.

In order to insure a local maximum, we need condition (A.6). Taking the derivative of (A.8) at t = 0 gives

36

$$\frac{\partial^2 \log Q(t)}{\partial t^2}\Bigg|_{t=0} = \frac{\bar{N}^2 \, \text{Tr}\left(2\,[G]\,[\hat{B}]\,[\check{\mathcal{R}}_0]\,[\hat{B}]^t\,[G]^t\right)}{\delta(0)} - \frac{\vec{N}^4 \, \text{Tr}\left(2\,[H_{MQ}]\,[\hat{B}]\,[\check{\mathcal{R}}_0]\,[\hat{B}]^t\,[G]^t\right)}{\delta^2(0)}$$

$$- \frac{\text{Tr}\left(2\,[G]\,[D]\,[G]^t\right)}{\delta(0)} + \frac{\text{Tr}\left(2\,[H_{MQ}]\,[D]\,[G]^t - 2k\bar{N}^2\,[G]\,[\hat{B}]\,[\check{\mathcal{R}}_0]\,[\hat{S}]^t\right)}{\delta^2(0)}\;.$$

(A.13)

After some manipulation, we have

$$\frac{\partial^2 \log Q}{\partial t^2}\Bigg|_{t=0} = - \frac{2\bar{N}Q_{max}\,\text{Tr}\left([G]\left(\left[\begin{smallmatrix} & & 0 \\ & [\hat{B}]\,\hat{\underset{\sim}{0}} & \\ 0 & & \end{smallmatrix}\right] + \left(\frac{Q_{max}-1}{Q_{max}}\right)\bar{N}[\hat{B}]\,[\check{\mathcal{R}}_0]\,[\hat{B}]^t\right)[G]^t\right)}{\delta(0)}$$

$$- \left(\begin{array}{c}\text{Matrix}\\\text{expression}\end{array}\right)\cdot\left(\frac{\partial \log Q}{\partial t}\Bigg|_{t=0}\right)$$

(A.14)

where we have recognized the last factor as the first derivative at $t=0$.
Finally, using (A.6) with (A.14) gives the condition

$$- \frac{2\bar{N}Q_{max}\,\text{Tr}\left([G]\left(\left[\begin{smallmatrix} & & 0 \\ & [\hat{B}]\,\hat{\underset{\sim}{0}} & \\ 0 & & \end{smallmatrix}\right] + \left(\frac{Q_{max}-1}{Q_{max}}\right)\bar{N}[\hat{B}]\,[\check{\mathcal{R}}_0]\,[\hat{B}]^t\right)[G]^t\right)}{\delta(0)} < 0 \qquad \forall[G]\;.$$

(A.15)

This condition is insured if and only if

$$\left[\begin{smallmatrix} & & 0 \\ & [\hat{B}]\,\hat{\underset{\sim}{0}} & \\ 0 & & \end{smallmatrix}\right] + \frac{Q_{max}-1}{Q_{max}}\,\bar{N}[\hat{B}]\,[\check{\mathcal{R}}_0]\,[\hat{B}]^t > [0]\;. \qquad (A.16)$$

37

Thus, if conditions (A.9) and (A.15) are met, we can be assured of a filter $[H_{MQ}]$ which will produce a local maximum in Q.